Short time properties, dynamic fragility and pressure effects in deeply supercooled polymer melts

2007 J. Phys.: Condens. Matter 19 205123

(http://iopscience.iop.org/0953-8984/19/20/205123)

IOP PUBLISHING JOURNAL OF PHYSICS: CONDENSED MATTER

J. Phys.: Condens. Matter **19** (2007) 205123 (13pp) doi:10.1088/0953-8984/19/20/205123

Short time properties, dynamic fragility and pressure effects in deeply supercooled polymer melts

Erica J Saltzman and Kenneth S Schweizer

Department of Materials Science, University of Illinois, 1304 West Green Street, Urbana, IL 61801, USA

E-mail: kschweiz@uiuc.edu

Received 1 October 2006
Published 25 April 2007
Online at stacks.iop.org/JPhysCM/19/205123

Abstract

Our activated barrier hopping theory of segmental relaxation in deeply supercooled polymer melts is applied to compute short time properties including the glassy shear modulus, localization length and vibrational frequency. Numerical calculations for specific polymers suggest the theory simultaneously predicts a reasonable elastic modulus, localized state vibrational frequency, dynamic fragility and dynamic crossover and glass transition temperatures. The theory also provides explicit connections between short time-/length-scale properties and the slow alpha relaxation process. The extension of the theory to elevated pressures is initiated. Pressure is found to broaden the deeply supercooled regime and reduce the dynamic fragility. However, the predicted Rossler–Sokolov universal supra-Arrhenius law for the temperature dependence of the alpha relaxation time remains accurate at all pressures. A common theme is the essential role played by the ratio of the dynamic crossover temperature (ideal mode coupling critical temperature) and kinetic glass transition temperature even in the deeply supercooled regime where activated processes are dominant.

(Some figures in this article are in colour only in the electronic version)

1. Introduction

Fundamental understanding of slow dynamics in deeply supercooled liquids is a major challenge, continuing to spawn diverse theoretical approaches that remain strongly debated [1]. In the polymer field the tension between thermodynamic versus kinetic based approaches has a long history, with the entropy catastrophe and free volume models representing the classic extremes. Idealized mode-coupling theory (MCT) [2] is a powerful dynamic approach formulated at the fundamental level of forces. A primary result is the prediction of an ideal nonergodicity or glass transition at a temperature, T_c, well above the experimental

vitrification temperature T_g. A common interpretation of the MCT critical temperature is that it signals a smooth crossover to strongly activated dynamics [2, 3], for which there exists ample experimental evidence at an empirically deduced temperature $T_c \sim (1.1\text{–}1.4)T_g$ [1, 4]. Recently we presented a microscopic kinetic approach to address this problem for hard sphere fluids and suspensions [5] and polymer melts [6] built on ideas from naïve ideal mode coupling [7], dynamic density functional [8] and activated rate theories [9]. The polymer theory focuses on activated barrier hopping below T_c, and was developed with the goals of simplicity, minimizing adjustable parameters and optimizing predictability. This motivated modest coarse graining to the segmental level corresponding to the (nontraditional within MCT) idea that dynamic collective density fluctuations on length scales considerably *longer* than the local cage scale control slow dynamics in the deeply supercooled regime. The goals of this paper are to work out predictions of the theory for short time properties, investigate their relation with the slow alpha relaxation, and initiate generalization of the approach to high pressures. A unifying theme is the critical role played by the ratio T_c/T_g, which both quantifies the breadth of the deeply supercooled regime and emphasizes the fundamental importance of the dynamic crossover (or ideal MCT) temperature.

We begin by briefly reviewing in sections 1 and 2 our prior work [6]. New calculations of the dynamic fragility are also given in section 2. Section 3 presents new results for short time dynamic properties associated with the quasi-localized state. The effect of pressure on T_c, T_g and the alpha relaxation time is addressed in section 4. The paper concludes with a brief discussion in section 5.

For polymer melts the elementary object of our theoretical description is a coarse grained 'statistical segment' of size σ. The *dynamical* consequences of chain connectivity are ignored, corresponding to treating the melt as a liquid of segments. Neglect of global connectivity is justified for the local segmental relaxation process at all temperatures of interest ($T_c > T > T_g$) given the experimental fact that glassy dynamics becomes chain length independent for long enough polymers. Of course, local chain structure (backbone stiffness, monomer shape, rotational isomerism) is important at a quantitative, material-specific level. However, a first principles treatment of the *dynamical* consequences of such chemical aspects is a formidable task and hence we adopt the simplest locally coarse grained 'Gaussian thread' chain model (degree of polymerization N) [10]. The closed nonlinear stochastic Langevin equation of motion for the instantaneous scalar *displacement* of a segment from its initial ($t = 0$) location, $r(t)$, is [5, 6]

$$M\frac{\partial^2 r(t)}{\partial t^2} = -\zeta_s\frac{\partial r(t)}{\partial t} - \frac{\partial F_{\rm eff}[r(t)]}{\partial r(t)} + \delta f(t) \tag{1}$$

where M is the mass, the random force satisfies $\langle \delta f(0)\delta f(t)\rangle = 2k_BT\zeta_s\delta(t)$, and ζ_s is a short time friction constant. The nonequilibrium free energy consists of ideal entropy and caging-like contributions

$$\beta F_{\rm eff}(r) = -3\ln(r) - \int \frac{d\vec{q}}{(2\pi)^3}\rho C^2(q)S(q)[1+S(q)]^{-1}\exp\left\{-\frac{q^2r^2}{6}[1+S^{-1}(q)]\right\} \tag{2}$$

where $\beta \equiv (k_BT)^{-1}$. For long Gaussian threads the pre-averaging over local structural and interaction potential length scales results in a wavevector-independent site–site direct correlation function $C(q) = C_0$, and a collective structure factor $S^{-1}(q) = S_0^{-1} + \frac{1}{12}q^2\sigma^2$, where $S_0 \equiv S(q=0) = \rho k_BT\kappa = (-\rho C_0)^{-1}$ is the dimensionless compressibility which quantifies the amplitude of long wavelength thermal density fluctuations, the statistical segment length $\sigma = \sqrt{C_\infty}l$ where l is the average length of a backbone chemical bond and C_∞ is the characteristic ratio, and $\rho\sigma^3$ is the reduced segmental density, which is of order unity. Using

these results, simple algebra and appropriate nondimensionalizations allows the nonequilibrium free energy to be written as [6]

$$\beta F_{\rm eff}(\alpha^*) = \frac{3}{2}\ln(\alpha^*) - \frac{12\sqrt{3}}{\pi}\lambda\int_0^\infty {\rm d}y\left(\frac{y}{1+y^2}\right)^2 \exp\left[-\frac{y^2(1+y^2)}{4\alpha^*}\right] \quad (3a)$$

$$\lambda \equiv \frac{1}{\rho\sigma^3 S_0^{3/2}} \quad (3b)$$

where $y \equiv q\sigma\sqrt{S_0/12}$, $\alpha \equiv 3/2r^2$ and $\alpha^* \equiv \alpha\sigma^2 S_0^2/12$. The theory is characterized by a *single* dimensionless 'coupling constant', λ, involving *experimentally measurable* thermodynamic and structural quantities. This is the origin of its predictive power, which can be viewed as in the spirit of MCT, which predicts dynamics based solely on equilibrium input. Our quantification of force correlations and dynamic constraints based on a thermodynamic property (S_0) would appear to be in contrast with theories based on the 'entropy crisis' idea, including the modern entropic droplet approach [11] and molecularly sophisticated formulations for polymers [12], which effectively *a priori* postulate a connection between a configurational entropy and a barrier hopping controlled relaxation time in the Adams–Gibbs–diMarzio spirit [1]. Note that the shape and characteristics of the nonequilibrium free energy of equation (3) are not universal given the material specificity of $\rho\sigma^3$ and S_0.

Minimization of the nonequilibrium free energy with respect to r, or dropping the thermal noise term in equation (1), yields a self-consistent localization equation for the 'naïve' MCT glass transition which occurs at $\lambda_{\rm c} = 8.32$. A polymer integral equation theory analysis suggests a simple temperature dependence for S_0 which has been demonstrated to describe experimental data extremely well [6]:

$$S_0^{-1/2} = -A + (B/T) \quad (4)$$

where $A > 0$ and B is related to the melt cohesive energy. The material-, pressure- and (in principle) degree-of-polymerization-dependent parameter A is of order unity, and typically $B \sim 700$–1300 K and correlates with polymer polarity. Combining equations (3) and (4), and taking the segmental density as a material constant, yields

$$T_{\rm c} = \frac{B}{A + (\lambda_{\rm c}\rho\sigma^3)^{1/3}}. \quad (5)$$

A priori calculation of $T_{\rm c}$ for many real polymers yields numerically realistic values [6]. Below $T_{\rm c}$ ($\lambda > \lambda_{\rm c}$) there is a smooth crossover to the deeply supercooled regime where collective barriers due to segment–segment interchain forces emerge. Figure 1 shows a typical result for the nonequilibrium free energy, which is characterized by a metastable local minimum and a barrier of height $F_{\rm B}$. Numerical calculations find the barrier is extremely well described (see inset) by a critical power law form:

$$\beta F_{\rm B} \approx c(\lambda - \lambda_{\rm c})^{\Delta}, \qquad c \cong 0.4, \qquad \Delta \simeq 1.3. \quad (6)$$

Although the barrier height is a universal function of the dimensionless coupling constant, its *temperature* dependence is material specific.

Above $T_{\rm c}$ the dynamics is treated in an Arrhenius manner (consistent with experiment) corresponding to a 'primitive' [1] alpha relaxation time $\tau_0(T) \equiv \tau_0 \exp(\varepsilon/k_{\rm B}T)$ where $\tau_0 \approx 10^{-14\pm1}$ s is a vibrational timescale and ε is a material-specific local activation energy. Below $T_{\rm c}$ the simplest model that smoothly bridges the normal and supercooled regimes is employed [6]:

$$\tau(T) = \tau_0 \exp\left(\frac{\varepsilon}{k_{\rm B}T}\right)\exp\left(\frac{a_{\rm c}F_{\rm B}(T)}{k_{\rm B}T}\right). \quad (7)$$

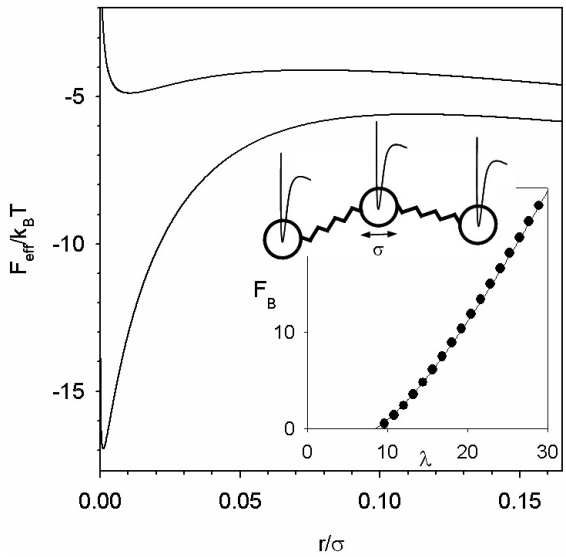

Figure 1. Nonequilibrium free energy (units of thermal energy) as a function of dimensionless displacement for parameters appropriate for polyvinylacetate (PVAC) [6]. Top (bottom) curve: $\lambda = 10$ and $T_c/T = 1.04$ ($\lambda = 20$ and $T_c/T = 1.27$). Upper inset: schematic diagram of localized polymer segments connected by entropic springs. Lower inset: collective barrier (units of k_BT) as a function of the coupling constant λ. Numerical results (points) are fitted by the critical power law of equation (6).

This corresponds to adopting the primitive alpha timescale as the dynamical prefactor for hopping over collective barriers. As previously discussed [6], equation (7) ignores a narrow intermediate temperature crossover regime that may often bridge the Arrhenius and deeply supercooled regimes.

Recall that underlying equation (1) is a 'segmental liquid' model corresponding to the simplifying assumption that global chain connectivity does not modify the barrier hopping process. In reality there are short range equilibrium correlations between connected segments that have dynamic consequences. To *empirically* model this effect a temperature-*independent* cooperativity parameter, a_c, is introduced in equation (7) corresponding to an effective barrier height of $a_c F_B$ [6]. Physically, a_c should correspond to the number of dynamically correlated segments along the chain, and therefore its magnitude is determined by a dynamical correlation length. The latter is typically assumed to be reliably estimated from an equilibrium measure of chain backbone stiffness: either the Kuhn length $l_k = C_\infty l$, or the persistence length $\xi_p = (C_\infty + 1)l/2$ [13, 14]. For the Gaussian thread model the cooperativity parameter can be determined by equating the end-to-end distance of the dynamically cooperative unit ($\sqrt{a_c}\sigma$) to the Kuhn or persistence length, thereby yielding $a_c = C_\infty$ or $a_c = (C_\infty+1)^2/4C_\infty$, respectively. Since typically $C_\infty \approx$ 4–10, estimates of $a_c \sim$ 1–10 follow. The characteristic ratio generally increases with chain length, ultimately saturating at a material-specific value of N [15]. This implies the intuitive trend of a finite size increase of the cooperativity parameter as chains get longer.

The material-specific local activation energy is not *a priori* known and is determined by adopting the recent proposition [16] of a (nearly) universal 'magic relaxation time' at the dynamical crossover $\tau_0(T_c) \cong 10^{-7\pm1}$ s. A qualitative argument for its physical basis has been given [6]. This condition plus equation (3) then yields (for $\tau_0 \approx 10^{-14}$ s) $\varepsilon \cong (16.1 \pm 2.5) k_B T_c$.

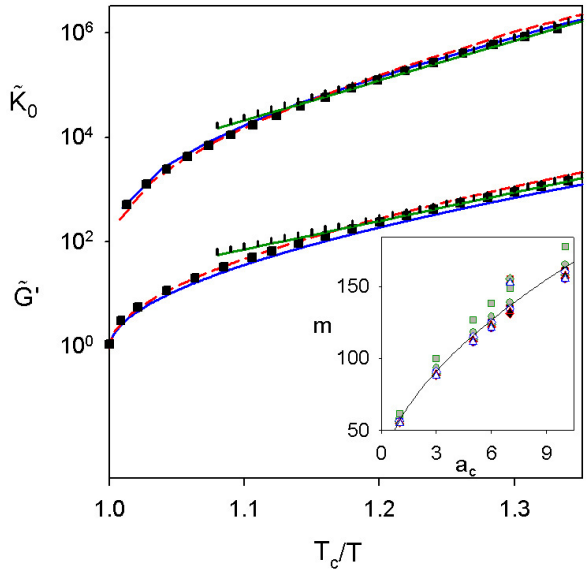

Figure 2. Dimensionless spring constant (units of $k_B T/\sigma^2$; upper group) and glassy shear modulus (units of $k_B T/\sigma^3$; lower group) as a function of inverse dimensionless temperature for polymer parameters representative of [6] PVAC (solid blue curve), polyetherimide (PEI) (dashed red curve) and polypropylene (PP) (squares). Hatched green lines are exponential fits. Inset: dynamic fragility at the glass temperature ($\tau(T_g) \equiv 100$ s, $\tau(T_c) \equiv 10^{-7}$ s, material parameters from [6]) as a function of cooperativity parameter for PS (filled red circles), PMMA (shaded green circles), polybutadiene (open blue circles), polyethyleneoxide (filled red squares), PEI (shaded green squares), polyethylene (open blue squares), polydimethylsiloxane (filled red diamonds), polycarbonate (shaded green diamonds), PP (open blue diamonds), PVAC (filled red triangles), polyisobutylene (shaded green triangles), polyisoprene (open blue triangles). The single curve is a collective fit given by $m = 16 + 40.6 a_c^{0.56}$, where the intercept was forced to agree with the $a_c = 0$ noncooperative Arrhenius behaviour.

Equations (3)–(7) constitute our analytic theory for the alpha relaxation time in the deeply supercooled regime. The practical experimental criterion for a glass transition is $\tau(T_g) = 10^x$ s where $x = 2$–4.

2. Dynamic fragility

The theory sketched in section 1 is divergence free. It predicts temperature dependences of the alpha time consistent with experimental analyses based on empirical multi-parameter functional forms generally involving (hypothetical) essential singularities such as the free volume or Vogel–Fulcher–Tammann (VFT) equations [6]. The inset of figure 2 shows new calculations of the dynamic fragility, $m \equiv \mathrm{d}(\lg \tau)/\mathrm{d}(T_g/T)|_{T_g}$, which establish how it grows with the cooperativity parameter. Since the equation of state properties of most polymers are quite similar (segment density, A and B in equation (4)), the origin of the large range of dynamic fragilities (∼45–180) observed for polymers is suggested to arise primarily from intrachain constraints (stiffness) as encoded in the parameter a_c. Our prior analytic and numerical analysis reveals a fundamental connection between the fragility and the ratio of the crossover to kinetic glass temperatures which quantifies the breadth of the deeply supercooled regime [6]:

$$m \cong b/[1 - (T_g/T_c)] \tag{8}$$

where $b \approx 14 \pm 2$ for $\tau(T_c) = 10^{-7\pm1}$ s and $\tau(T_g) = 100$ s. This correlation is in excellent agreement with experiment [17]. Equation (8) also corresponds to a close relationship between the local activation energy (or T_c) and fragility. This connection between short and long time dynamical processes has been recently emphasized experimentally [18]. Additionally, since the characteristic ratio (and hence a_c) generally decreases as chains get shorter, T_g decreases more strongly than T_c as N is reduced, and hence the breadth of the supercooled regime is expected to increase as N decreases. Equation (8) then immediately implies the dynamic fragility decreases as chains get shorter, a trend often observed [19, 20]. It also suggests that what controls the long chain limit of the dynamic fragility is the saturation of the characteristic ratio ($C_N \to C_\infty$) corresponding to the attainment of full Gaussian statistics, as emphasized by Sokolov *et al* based on experimental studies [15].

A universal form for the temperature dependence of the alpha relaxation time in the deeply supercooled regime of a supra-exponential critical power law form has been previously shown to be predicted based on approximate analytic analysis and detailed numerical calculations [6]:

$$\begin{aligned} &\mathrm{Lg}[\tau(T)/\tau(T_c)] = cX^\nu \\ &X \equiv [(T_c/T) - 1]/[(T_c/T_g) - 1] \end{aligned} \tag{9}$$

where X is a normalized and dimensionless inverse temperature variable that quantifies the distance from the dynamic crossover and onset of collective barriers. The effective exponent $\nu \cong 1.4 \pm 0.1$ depends weakly on the dynamic crossover time and temperature range analysed, and c is a constant. Equation (9) corresponds to a nonanalytic supra-Arrhenius temperature dependence that transcends *all* material details of the theory (segmental density, compressibility parameters A and B, cooperativity parameter, etc). Its basic form, including the magnitude of effective exponent, is in excellent accord with experiments on a wide range of glassy materials including polymer melts [17].

3. Short time properties

A (perhaps overly) stringent test of our coarse grained segment level theory is whether it makes reasonable predictions for short time properties such as the glassy elastic shear modulus, G', and localized state vibrational frequency. These properties are controlled not by the slow barrier hopping process, but rather the nature of the quasilocalized state. As evident in figure 1, the localization length (minimum of $F_{\mathrm{eff}}(r)$) obeys $r_{\mathrm{loc}} \ll \sigma$ and decreases with cooling. The barrier location is weakly temperature dependent and of the order of a few tenths of a segment length. As indicated by the schematic diagram in figure 1, such short lengths seem qualitatively consistent with our use of a 'liquid of segments' model in the sense that barrier hopping occurs on distance scales significantly smaller than those associated with entropy-driven conformational fluctuations on length scales larger than the statistical segment length (Rouse or entangled dynamics [21]). Indeed, this is the fundamental assumption of all the classic coarse-grained theories for the universal chain dynamics [21] which treat the glassy relaxation process as merely defining a local segmental friction constant which sets the elementary timescale for large scale polymer motions. In this section we analyse glassy mechanical and vibrational properties and their connection to the long time alpha process.

3.1. Localized state vibrational frequency

Below T_c the minimum of $F_{\mathrm{eff}}(r)$ is characterized by its harmonic curvature or spring constant, $K_0(T)$. Numerical calculations of this quantity for three polymers are shown in figure 2. The

spring constant rises rapidly near the crossover temperature and then exhibits an Arrhenius dependence: $\tilde{K}_0 \approx K_0\sigma^2/k_BT \propto \exp(bT_c/T)$ with $b \sim 17$–18. The material dependence is weak. As previously discovered for athermal hard sphere fluids [5], we find (not plotted) that for values of βF_B up to $\sim$10 there is a direct correlation of the spring constant and barrier height given roughly by $\beta F_B \propto \sqrt{\tilde{K}_0}$. This is an intriguing result since it implies a tight connection between the property that controls long time relaxation (barrier) and one that controls short time vibrational motion.

From a solid state perspective our single particle Langevin equation theory is of the form of a simple damped Einstein oscillator model at short times. The analogue of a boson peak type excitation corresponds to a localized underdamped oscillatory solution of equation (1). The dissipative short time/distance dynamics enter equation (1) enter via a friction constant. For motion on very short length- and timescales this corresponds to the ubiquitous 'fast beta' process, a *non*-activated Debye process which exhibits a nearly temperature- and material-independent relaxation time of the order of a picosecond [1, 22, 23]. Here we simply examine the characteristic timescales of the Brownian harmonic limit of equation (1), which is given by

$$M\frac{\partial^2 r(t)}{\partial t^2} + \zeta_s\frac{\partial r(t)}{\partial t} + K_0(r(t) - r_{loc}) = \delta f(t). \tag{10}$$

Analytic solution of this linear stochastic differential equation is standard. The damped harmonic oscillator relaxation time is $\tau_s = 2M/\zeta_s$, and the circular frequency is

$$\Omega_B = \frac{1}{2\pi}\sqrt{\frac{K_0}{M}}\left[1 - \frac{M}{K_0}\left(\frac{\zeta_s}{2M}\right)^2\right]^{1/2} \equiv \frac{\Omega_{B,0}}{2\pi}\sqrt{1-R} \tag{11}$$

where $R \equiv (\Omega_{B,0}\tau_s)^{-2}$. These results apply in the underdamped regime corresponding to $R < 1$. Since R decreases as temperature is lowered (see below) the above frequency grows with cooling, ultimately saturating at $\Omega_{B,0}$. Experiments do suggest the boson peak frequency increases with cooling [26]. Whether the saturation occurs above T_g requires a precise calculation.

It is of interest to numerically estimate $\Omega_{B,0}$ based on the experimental knowledge that $\tau_s \approx$ ps and our theoretical results for K_0. Interestingly, recent experiments on polymethylmethacrylate (PMMA) find the observable features of the boson peak are qualitatively the same for incoherent (single particle) and coherent (collective) inelastic scattering [24], suggesting our self-localization model has some merit for this property. The effective mass involved in the polymer boson peak phenomenon remains debated, but $\sim$5–10 monomers has been suggested. Experiments on polymers [22], and also van der Waals molecular glass formers [25], have reported a simple inverse square root dependence of the boson peak frequency on mass, which is in qualitative accord with equation (11) when R is small.

For polystyrene (PS) or PMMA, the Kuhn length corresponds to roughly ten backbone bonds or five monomers. Taking this as the mass, $\sigma = \sqrt{C_\infty}l \approx 0.5$ nm and $T_c/T_g \sim 1.13$ (corresponding to a fragility of $\sim$115–120), equation (11) yields an upper bound for Ω_B at the glass transition of $\Omega_{B,0} \sim 1500$ GHz. The boson peak of many polymers falls in the range of 1.3–4 meV $\sim$300–1000 GHz. Obviously, choosing a larger effective mass reduces the theoretical result, as would corrections due to nonzero R. Since $R \equiv 1/(\Omega_{B,0}\tau_s)^2 \propto K_0^{-1} \propto \exp(-bT_c/T)$, we are led to the suggestion (all other factors being the same) that the localized state vibrational frequency increases for less fragile systems corresponding to larger T_c/T_g values. As T_c is approached the nonequilibrium free energy loses its localized state (minimum) and one expects a crossover to an overdamped (nonoscillatory) short time

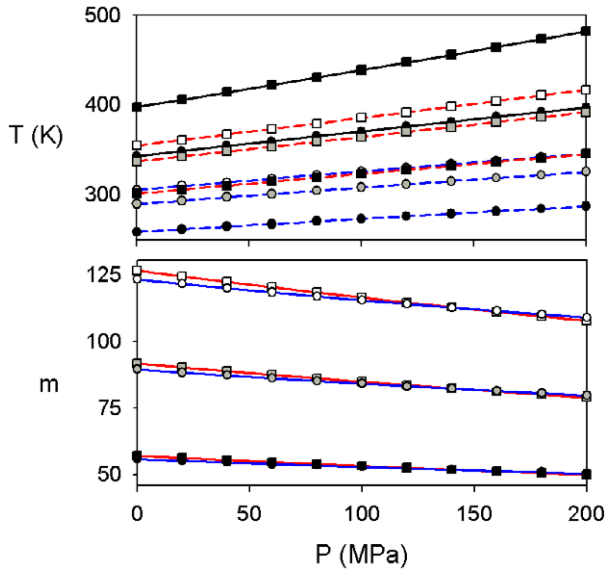

Figure 3. Top panel: dynamic crossover and glass transition temperatures as a function of pressure ($\tau(T_g) \equiv 100$ s, $\tau(T_c) \equiv 10^{-7}$ s). Lines with squares are for polystyrene (PS); circles are for PVAC. Dynamic crossover (or ideal MCT) temperatures are solid lines and glass transition temperatures are dashed lines (PS—red, PVAC—blue) with $a_c = 1, 3, 6$ (filled, shaded, open shapes). Lower panel: dynamic fragility at $T_g(P)$ as a function of pressure for PS and PVAC. Symbols and lines as above.

dynamics corresponding to $R > 1$. Using $\tau_s \approx$ ps, our calculations of K_0, and the above PMMA material parameters, we estimate from the condition $R(T^*) = 1$ that this crossover temperature T^* lies just below T_c.

As a cautionary comment, we realize that the physics underlying the boson peak no doubt involves some degree of collective vibrational motion of many elementary units although the details remain poorly understood [1, 22–27]. Our single particle or Einstein solid approach ignores such cooperative motion. However, the recent incoherent scattering experiments on PMMA [24] are suggestive that local self-motion may faithfully reflect crucial aspects of the collective vibrational process quantified by the boson peak measurements.

3.2. Glassy shear modulus

The standard Green–Kubo formula for the elastic modulus is adopted, which, in conjunction with factorization of multipoint correlations, yields the glassy shear modulus due to segmental localization [28]

$$G' = \frac{k_B T}{60\pi^2} \int_0^\infty dq \left(q^2 \frac{\partial}{\partial q} \ln S(q) \right)^2 \exp\left[-\frac{q^2 r_{loc}^2}{3S(q)} \right]. \tag{12}$$

The modulus is determined by the dimensionless compressibility, segmental density and localization length, r_{loc}. Figure 3 shows results for G' in units of $k_B T/\sigma^3$. The modulus at the onset of segmental localization is $\tilde{G}' \equiv \sigma^3 G'/k_B T_c \approx 1$. Interestingly, since $\rho\sigma^3 \approx 1$ [6] this implies $G'(T_c) \approx \rho k_B T_c = G'_{Rouse}$, where G'_{Rouse} is the zero time initial Rouse theory shear modulus associated with the *intrachain conformational entropy* of a Gaussian coil [21]. Hence, upon cooling below T_c the modulus due to *inter*chain interactions and transient

segment localization becomes significant relative to the high temperature entropic contribution. Such enhanced elasticity has long been known to exist in polymer melts [29], and its onset historically defines a temperature $T_{ll} \approx (1.2 \pm 0.1)T_g$. This observation finds a natural and fundamental theoretical basis in our approach where $T_{ll} \approx T_c$, as also suggested by Sokolov and co-workers [30].

From figure 2 one sees that deep in the supercooled regime the glassy modulus grows exponentially with cooling in a weakly material-specific manner, $\tilde{G}' \propto \exp(aT_c/T)$, where $a \sim 12$–13. This temperature dependence is considerably stronger than for the bulk modulus, $K_B = \rho k_B T S_0^{-1}$, but weaker than for the spring constant K_0. At the glass temperature, using $\sigma \simeq \sqrt{C_\infty} l \quad \sim 0.5$ nm, $T_c/T_g \sim 1.13$ and $T_g \sim 345$–350 K characteristic of PS and PMMA, figure 2 implies that $\tilde{G}' \approx 60$–70, which corresponds to $G' \sim 2.5$–3 GPa. Experimentally, the order of magnitude of the glassy polymer modulus at T_g is 1–3 GPa [31].

Without overemphasizing the numerical aspects, we believe the ability of our theory to simultaneously predict a reasonable elastic modulus, localized state vibrational frequency, dynamic fragility, the scaling of equation (9) and crossover temperature and glass temperatures is significant. It also provides an explicit theoretical realization of a strong correlation between short time/length-scale properties and the slow alpha relaxation process as commonly observed experimentally [1, 16].

4. Pressure effects

The development of our theory thus far has focused entirely on the dynamics as a function of temperature at atmospheric pressure. External pressure also enters the theory via the dimensionless compressibility and segmental density in equation (3). Our present goal is to briefly investigate at a zeroth order level the nature and sensitivity of our theory for pressure effects, a detailed treatment of which will be the subject of a future publication. By far the most pressure-sensitive property is the isothermal compressibility, which decreases quite strongly with pressure. We employ the experimental finding that the bulk modulus of polymer melts and molecular liquids is to a good approximation linearly dependent on pressure: $K_B(P) \cong K_B(P = 0) + B_1 P$, where B_1 is a material specific constant, typically ~8–12 for polymers [33]. The dimensionless compressibility can then be written as

$$\frac{1}{S_0(T,P)} = \frac{1}{S_0^0(T)} + \frac{B_1 P}{\rho k_B T} = \left(-A + \frac{B}{T}\right)^2 + \frac{P}{P_1} \tag{13}$$

where $P_1 \equiv \rho k_B T/B_1$ and $S_0^0(T) \equiv S_0(T,0)$ is the atmospheric pressure dimensionless compressibility. Recent experiments have found the dynamic crossover time is pressure independent [32], a result we adopt literally. For analytic simplicity, σ and $\rho\sigma^3$ are taken as T- and P-independent material parameters while allowing $\rho = \rho(P,T)$ to vary according to the equation of state. There must be corrections to the above simplifying assumptions but they require polymer-specific experimental data to assess.

Equation (13) implies that S_0^{-1} remains a quadratic function of inverse temperature, and the nonequilibrium free energy continues to be specified by the dimensionless coupling constant of equation (3). Hence all the prior analytic and numerical analysis of the theory at atmospheric pressure [6] carries over to the high pressure regime. The dynamic crossover temperature occurs at $\lambda = \lambda_c = 8.32$. Combining equations (3*b*) and (13) thereby yields

$$\frac{T_c(P)}{B} = \left\{ A - \frac{P}{2\tilde{P}_2} + \sqrt{D - A\frac{P}{\tilde{P}_2} + \left(\frac{P}{2\tilde{P}_2}\right)^2} \right\}^{-1}$$
$$T_c(P) \cong T_c^0 \left\{ 1 + \frac{T_c^0 P}{2B\tilde{P}_2}\left(1 + \frac{A}{\sqrt{D_c}}\right)\right\} \tag{14}$$

where $(S_{0,c})^{-1} = (\lambda_c \rho\sigma^3)^{2/3} \equiv D_c$ and $\tilde{P}_2 \equiv \rho k_B B/B_1$. The second line is the leading order in pressure result where T_c^0 is given by equation (5). If the temperature is fixed at $T > T_c^0$ then the crossover pressure is

$$P_c = \frac{\rho k_B T}{B_1}\left[D_c - \left(\frac{B}{T} - A\right)^2 \right]. \tag{15}$$

Although not pursued here, by following prior analysis [6] approximate (but accurate) analytic results can be derived for $T_g(P)$, the breadth of the supercooled regime, $T_c(P)/T_g(P)$, and the fragility $m(P)$.

In our model calculations the quantities $\rho k_B T$ and $\rho(T, P)$ are computed using the equation of state that follows from equation (13) under the simplifying assumption of constant thermal expansivity for all temperatures, pressures and materials. The parameter B_1 is treated as the single adjustable constant. Representative numerical results for the crossover and glass temperatures of PS and PVAC as a function of pressure are shown in figure 3 for several values of the cooperativity factor with fixed $\tau(T_g) = 100$ s and dynamic crossover time of 10^{-7} s. The parameter B_1 was chosen *once* for each polymer to reproduce the experimental value of $(dT_g/dP)_{P\to 0}$ (0.36 K MPa^{-1} for PS, 0.25 MPa K^{-1} for PVAC [32]) *when* $a_c = 3$, thereby yielding $B_1 = 3.15$ (2.54) for PS (PVAC). The pressure dependence of T_c and T_g are nearly linear. Hence the final equality in equation (14) provides insight into the factors that control the pressure dependence of the crossover temperature. Although not visually obvious, the pressure dependence of T_c is stronger than for T_g, and hence the breadth of the deeply supercooled regime increases with pressure.

Numerical calculations of the dynamic fragility at $T_g(P)$ for all model parameters and pressures are found to be extremely well described by equation (8). Thus, as shown in figure 3, since the ratio T_c/T_g increases with pressure the fragility decreases with pressure in a manner that is quantitatively sensitive to polymer chemistry and the cooperativity parameter. Specifically, the calculations in figure 3 correspond to values of $dm/dP|_0$ between -0.05 and -0.1 (MPa)$^{-1}$. Figure 4 shows the relative percentage change of the fragility, $\hat{m} \equiv [m(P) - m(0)]/m(0)$, increases more slowly at elevated pressures, and is enhanced by increasing cooperativity parameter (a_c) and/or atmospheric fragility (PS versus PVAC). The trend of a pressure-induced reduction of fragility agrees with many, but not all, experiments on polymers [32]. For example, $dm/dP|_0 \approx -0.16$, -0.035, -0.18 and -0.5 (MPa)$^{-1}$ for PS, polybutadiene, PMMA and polyvinylchloride, respectively, but ~ 0 for PVAC and polymethylphenylsiloxane [32].

Insight concerning the origin of the strong nonuniversality of the pressure dependence of the fragility can perhaps be obtained from the general form of our theoretical result, which straightforwardly follows from equation (8):

$$\left.\frac{dm}{dP}\right|_0 = \frac{m_0^2}{b(1 - bm_0^{-1})}\frac{d}{dP}\lg\left(\frac{T_g}{T_c}\right)\bigg|_0 = \frac{b(T_c^0/T_g^0)}{[(T_c^0/T_g^0) - 1]^2}\frac{d}{dP}\lg\left(\frac{T_g}{T_c}\right)\bigg|_0. \tag{16}$$

A simple correlation of this pressure derivative with the atmospheric value of fragility (m_0), the dynamic crossover time, or another property is not evident [20]. However, in the context of our approach there is an underlying simplicity since the pressure derivative is fully specified by the ratio of the crossover to glass temperatures. The last factor in equation (16) suggests

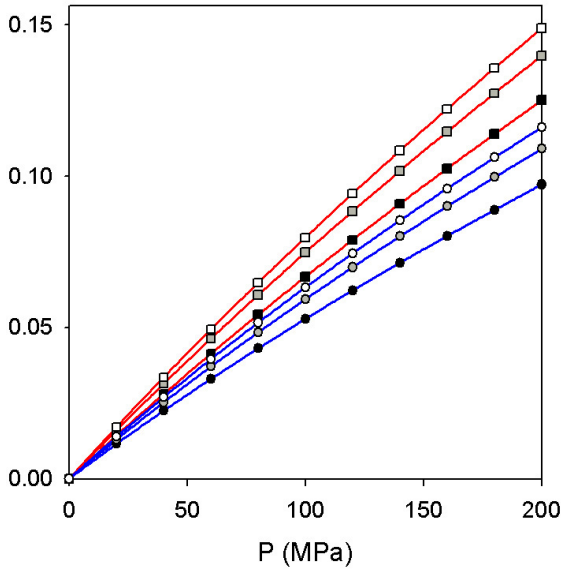

Figure 4. Normalized differential fragility, $\hat{m} \equiv [m(P) - m(0)]/m(0)$, as a function of pressure for the systems of figure 3.

subtle cancellation can occur, leading to pressure insensitivity of the fragility, if the *logarithmic* pressure derivatives of T_c and T_g are nearly equal. Equation (5) and our prior analytic expression [6] for the glass transition temperature provide explicit insight concerning what molecular factors enter. Note that an equation analogous to equation (16) can be written down for the molecular weight (N) derivative of the fragility. Since the cooperativity parameter is chain length dependent at low N via the characteristic ratio, an additional complexity is introduced in equation (16).

Finally, we have analysed the extent to which equation (9) applies at elevated pressures. Remarkably, the results in figure 5 show the universality predicted at atmospheric pressure [6] is equally accurate at elevated pressures for various polymers and cooperativity factors (at fixed dynamic crossover time). We remind the reader that equation (8) is an immediate consequence of equation (9). We believe the robustness of equation (9) is significant since it provides a unifying principle for how to understand, organize and create master plots of the temperature, pressure, chemical structure and molecular weight dependences of the alpha relaxation time. The critical material property is the *breadth of the deeply supercooled regime*, as quantified by the ratio T_c/T_g.

5. Summary

Our dynamical activated barrier hopping theory of segmental relaxation in deeply supercooled polymer melts [6] has been extended to treat short time properties (glassy shear modulus, localized state vibrational frequency), and their correlations with the dynamic fragility and alpha relaxation time have been established. Comparisons of the theory with experiments are encouraging. The extension of the theory to elevated pressures has been initiated. The theory predicts that pressure broadens the deeply supercooled regime and reduces the dynamic fragility. However, equation (9) remains remarkably accurate for fixed dynamic crossover time. For real materials the latter time is not strictly universal and hence system-specific deviations

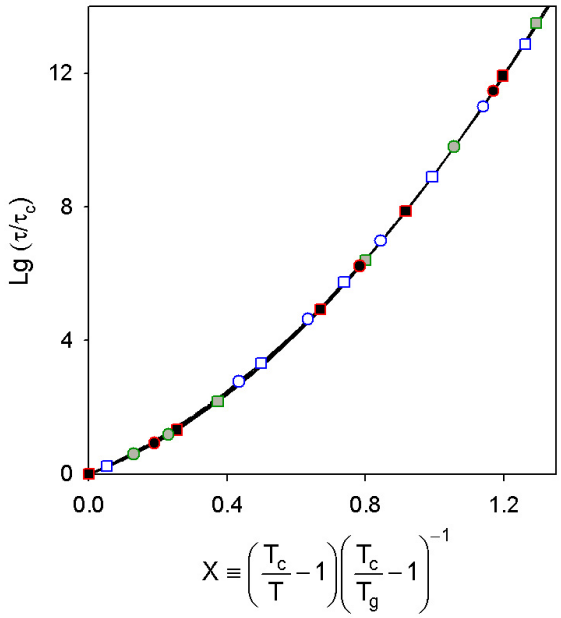

Figure 5. Logarithm (base 10) of the relaxation time normalized by the crossover time as a function of the dimensionless inverse temperature variable $X = (T_c/T - 1)/(T_c/T_g - 1)$ for temperatures from T_c to below T_g. Symbols indicate $a_c = 1$ (filled red), $a_c = 3$ (shaded green), $a_c = 6$ (open blue) for PS (squares) and PVAC (circles). Results at various pressures covering the range 0–200 MPa are shown. Fits to the form of equation (9) for the many different systems and pressures have been done, but on the scale of the plot all essentially collapse onto a single power law curve given by equation (9) with an effective exponent $\nu \approx 1.3$.

from the suggested master curve will occur [6]. The ratio of the dynamic crossover (ideal MCT) and glass temperatures plays a critical role in our results, which further supports prior findings [6] that T_c (and hence the ideal MCT nonergodicity transition) is an essential variable for controlling the activated barrier hopping process.

Related future research will work out the full predictions of the simple theory for the frequency domain boson peak-like feature, more carefully address pressure and chain length effects for specific polymers, and extend the theory to treat several types of dynamic heterogeneity effects driven by the barrier hopping process [28, 34]. Finally, there remains the major challenge of developing a unified theory that merges the present approach for glassy local segment dynamics (for which global chain motions are not important) with a description of coil scale polymer dynamics. Even for unentangled polymer melts the achievement of this goal requires a consistent treatment of intrachain (entropic spring) and interchain forces, and a more fundamental understanding of how the independent Rouse mode concept [21] emerges and its limitations. Experimental motivation for addressing this difficult problem includes the poorly understood, but ubiquitous and material-specific, phenomenon of the breakdown of time–temperature superposition in supercooled polymer melts [1, 30].

Acknowledgments

This work was supported by the US Department of Energy, Division of Materials Sciences, under award number DEFG02-91ER45439 through the Frederick Seitz Materials Research Laboratory. Helpful discussions with Alexei Sokolov are gratefully acknowledged.

References

[1] Ngai K L 2000 *J. Non-Cryst. Solids* **275** 7
Angell C A, Ngai K L, McKenna G B, McMillan P F and Martin S W 2000 *J. Appl. Phys.* **88** 3113
[2] Gotze W and Sjogren L 1992 *Rep. Prog. Phys.* **55** 241
[3] Bouchard J P, Cugliandolo L, Kuchan J and Mezard M 1996 *Physica* A **226** 243
Lowen H, Hansen J P and Roux J N 1991 *Phys. Rev.* A **44** 1169
Doliwa B and Heuer A 2003 *Phys. Rev.* E **67** 030501
Brumer Y and Reichman D R 2004 *Phys. Rev.* E **69** 041202
[4] Beiner M, Huth H and Schroter K 2001 *J. Non-Cryst. Solids* **279** 126
[5] Schweizer K S and Saltzman E J 2003 *J. Chem. Phys.* **119** 1181
Schweizer K S 2005 *J. Chem. Phys.* **123** 244501
[6] Schweizer K S and Saltzman E J 2004 *J. Chem. Phys.* **121** 1984
Saltzman E J and Schweizer K S 2004 *J. Chem. Phys.* **121** 2001
[7] Kirkpatrick T and Wolynes P G 1987 *Phys. Rev.* A **35** 3072
[8] Archer A J and Rauscher M 2004 *J. Phys. A: Math. Gen.* **37** 9325
Marconi M B and Tarazona P 1999 *J. Chem. Phys.* **110** 8032
[9] Kramers H A 1940 *Physica* **7** 284
[10] Schweizer K S and Curro J G 1997 *Adv. Chem. Phys.* **97** 1
[11] Xia X and Wolynes P G 2001 *Phys. Rev. Lett.* **86** 5526
Lubchenko V and Wolynes P G 2006 *Preprint* cond-mat/0607349
[12] Dudowicz J, Freed K F and Douglas J F 2006 *J. Chem. Phys.* **124** 064901
[13] Bershtein V A and Ryzhov V 1994 *Adv. Polym. Sci.* **114** 43
[14] Lodge T P and McLeish T C B 2000 *Macromolecules* **33** 5278
Inoue T and Osaki K 1996 *Macromolecules* **29** 1595
[15] Ding Y, Kisliuk A and Sokolov A P 2004 *Macromolecules* **37** 161
[16] Novikov V N and Sokolov A P 2003 *Phys. Rev.* E **67** 031507
[17] Rossler E and Sokolov A P 1996 *Chem. Geol.* **128** 143
Rossler E, Hess K U and Novikov V N 1998 *J. Non-Cryst. Solids* **223** 207
[18] Novikov V N and Sokolov A P 2004 *Nature* **431** 961
[19] Roland C M and Casalini R 2003 *J. Chem. Phys.* **119** 1838
[20] Huang D, Colucci D and McKenna G B 2002 *J. Chem. Phys.* **116** 3925
[21] Doi M and Edwards S F 1986 *Theory of Polymer Dynamics* (Oxford: Clarendon)
[22] Kanaya T and Kaji K 2001 *Adv. Polym. Sci.* **154** 88
[23] Colmernero J, Arbe A and Alegria A 1993 *Phys. Rev. Lett.* **71** 2606
Frick B and Richter D 1995 *Science* **267** 1939
[24] Kanaya T, Tsukusho I, Kaji K, Gabrys B J, Bennington S M and Furuya H 2001 *Phys. Rev.* B **64** 144202
[25] Renge I 1998 *Phys. Rev.* B **58** 14117
Yamamuro O, Tsukishi I, Matsuo T, Takeda K, Kanaya T and Kaji K 1997 *Prog. Theor. Phys. Suppl.* **126** 93
[26] Sokolov A P, Kisliuk A, Quitmann D, Kudlik A and Rossler E 1994 *J. Non-Cryst. Solids* **172–174** 138
[27] Ding Y, Novikov V N, Sokolov A P, Cailliaux A, Dalle-Ferrier C, Alba-Simionesco C and Frick B 2004 *Macromolecules* **37** 9264
[28] Schweizer K S and Saltzman E J 2004 *J. Phys. Chem.* B **108** 19729
[29] Boyer R F 1979 *Polym. Eng. Sci.* **19** 732
[30] Kisliuk A, Mathers R T and Sokolov A P 2000 *J. Polym. Sci.* B **38** 2785
[31] Ngai K L and Plazek D J 1995 *Rubber Chem. Tech. Rubber Rev.* **68** 376
[32] Roland C M, Hensel-Bielowka S, Paluch M and Casalini R 2005 *Rep. Prog. Phys.* **68** 1405
[33] Sanchez I C, Cho J and Chen W J 1993 *Macromolecules* **26** 4234
[34] Saltzman E J and Schweizer K S 2006 *J. Chem. Phys.* **125** 044509
Saltzman E J and Schweizer K S 2007 *Phys. Rev.* E **74** 06151